

THE COMBINED EFFECT OF COOLING SLOPE PLATE CASTING AND MOLD VIBRATION ON MICROSTRUCTURE, HARDNESS AND WEAR BEHAVIOR OF Al–Si ALLOY (A390)

M. M. Shehata, S. El-Hadad , and M. E. Moussa

Department of Casting Technology, Central Metallurgical Research and Development Institute, P.O. 87, Helwan, Egypt

M. El-Shennawy

Department of Mechanical Engineering, Faculty of Engineering, Helwan University, 1 Sherif St., P.O. 11795, Helwan, Egypt

Copyright © 2020 American Foundry Society
<https://doi.org/10.1007/s40962-020-00497-0>

Abstract

Semisolid casting using the cooling slope plate method (CSP) is known to refine the microstructure of hypereutectic aluminum alloys and enhance their mechanical properties. The current research investigates the combined effect of casting using the CSP and mechanical vibration of the mold on microstructure and wear behavior of A390 alloy. After pouring the alloy on the CSP, the mold (sand/metallic) was vibrated mechanically at 50 Hz during filling and up to solidification. Conventional casting with the same mold vibration conditions was also done for comparison. During CSP casting with mechanical vibration of the mold, the crystal nucleus multiplication inhibits the grain growth, and the dendrite break-up takes place simultaneously, leading to refinement of the microstructure. The double effect of the shear force by melt flow and vibrational turbulence is responsible for fragmentation of the particles. This finding was more pronounced in case of

using the sand mold. The quantitative measurements showed that the size of primary Si reduced from $\sim 184 \mu\text{m}$ for the conventional casting in the sand mold without vibration to $\sim 70 \mu\text{m}$ when the mold was vibrated and from $\sim 30 \mu\text{m}$ in case of CSP down to $\sim 20 \mu\text{m}$ when CSP was followed by mechanical vibration of the mold. However, applying the mechanical vibration after CSP in case of the metallic mold increased the size of primary Si from ~ 21 to $36 \mu\text{m}$. Accordingly, the improvement in the hardness and wear resistance of the CSP samples due to vibration was more significant in case of using the sand mold.

Keywords: cooling slope casting, mechanical vibration, microstructure, wear behavior

Introduction

In numerous different applications that require high abrasion resistance, high strength/weight ratio, resistance to corrosion, good mechanical properties, low thermal expansion and reduced density, hypereutectic Al–Si alloys such as A 390 are used. These features are the judicious choice for the aerospace and automotive industries to manufacture fuel-efficient vehicles using the light weight parts made from these alloys such as rods, pistons, air-compressors, cylinder liners and motor blocks.¹

The excellent properties of this group of alloys, specifically their wear resistance, are due to the presence of hard

primary silicon particles in the matrix. Therefore, these alloys may sometimes exhibit low mechanical properties which is caused by the harmful morphologies of primary Si particles, such as coarse polygonal, star-like, fish bone morphology, other irregular shapes and high-volume fraction of needle-like eutectic phase that are produced by the conventional casting. These negative effects limited the wider application of these alloys. Controlling the size, morphology and distribution of the primary silicon particles in hypereutectic Al–Si alloy castings is based on maximizing the number of nucleation sites and increasing nucleation rate, this nucleation phenomenon is commonly termed refinement.^{2,3}

The preferred practical choice for enhancing the mechanical properties of the hypereutectic alloys is to refine their microstructure by decreasing primary silicon size through different techniques. The refining processes can be classified into four categories: vibration and stirring refining (VS), rapid solidification (RS), chemical refining (CR) and severe plastic deformation (SPD). Among these methods, vibration is believed to enhance the microstructure by facilitating nucleation process as concluded from various studies.⁴

The effect of mechanical vibration on A 356 alloy microstructure was investigated.⁵ Primary α -Al average size decreased and became smaller, as the degree of vibration increased. In a published study,⁶ conventional casting with vibration at 50 Hz for 15 min, the grain size of A356 reduced from 1200 μm to 174 μm . In order to minimize the α -Al grain size and the secondary dendritic arm spacing by increasing vibration frequency and amplitude, an efficient vibration method with greater solid fractions and a lower pouring temperature was introduced.⁷

Vibration treatment is also effective in promoting polyhedral crystal fracture, thus reducing the size of some complex structures and homogenizing their dispersion in the matrix.⁸ This is an important issue in case of the alloys containing complex intermetallic phases of some impurities such as iron, manganese, nickel or chromium.^{9,10} These compounds have various types, as thin needles or platelets, Chinese scripts, polyhedral and/or star-like crystals.^{11–13} The possible refinement of these phases by using different vibration techniques should be further investigated.⁴

Several research works were devoted to apply vibrations combined with semisolid casting. Some of these studies performed the semisolid casting by pouring the molten metal in the semisolid state into the mold cavity which is known as “rheocasting” and applying ultrasonic vibrations through ultrasonic system.^{14–17} It was found that rheocast aluminum alloy A380 exhibits finer grain size and fragmented Fe intermetallic particles when treated by ultrasonic vibrations at low pouring temperatures (620–640 °C).¹⁴ Modified microstructure and enhanced tensile strength of rheocast alloy A356 were obtained with

semisolid slurry under ultrasonic vibration for 50 s near its liquidus temperature.¹⁷

In contrast to ultrasonic vibration, mechanical vibration is still the most practical and more economical choice. However, the research work on the combined effect of semisolid casting with mechanical vibration is very limited. In a study for Gencalp and Saklakoglu,¹⁸ mechanical vibration was used to investigate its influence on the microstructure of cooling slope plate (CSP) cast AlSi8-Cu3Fe alloy and it was observed that the convection caused by the vibration in the course of solidification significantly reduces the grain size of α -Al. Other researchers also obtained very close results to this reported work.^{19–21}

In a recent research on hypereutectic A390 alloy prepared using CSP, well-refined primary Si particles were obtained and the optimum pouring temperatures were then determined for static mold conditions.²² In the current work, casting was carried out using the CSP method at the optimum pouring temperatures 690 °C and 710 °C for the metallic and the sand molds, respectively, obtained in,²² and then, the molds were mechanically vibrated during filling in order to study the combined effect of both CSP and vibration on the microstructure (size and distribution of primary Si), hardness and wear behavior of an Al–Si alloy (A390).

Materials and Experimental Procedures

Aluminum silicon alloy, A390 with the chemical composition shown in Table 1 was prepared using pure aluminum. The other additives were charged into the furnace as pure metals include Si, Cu, Mn and Mg, while Ti was added as Al-10 wt% Ti master alloy. Melting was done in 100 kg capacity medium-frequency induction furnace. The pouring temperatures in the present work were selected relative to the liquidus temperature of the alloy according to the differential scanning calorimetric (DSC) analysis of 650 °C from the previous research.²² The optimum pouring temperatures in the current experimental work were selected based on the previous research²² to be 690 °C and 710 °C for the metallic and sand molds, respectively.

Table 1. Chemical Composition of the Prepared Alloy (wt%) and the ASTM B179 Standard Composition limits of A390

Alloy	Si	Cu	Mg	Fe	Mn	Zn	Ti	Al
Alloy A390								
Min.	16.0	4.0	0.5	–	–	–	–	Bal
Max.	18.0	5.0	0.65	0.4	0.1	0.1	0.2	
Prepared alloy	17.4	3.97	0.60	0.22	0.076	0.09	0.1	Bal

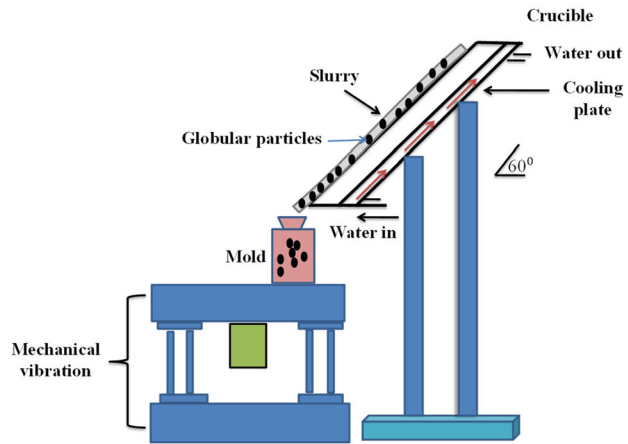
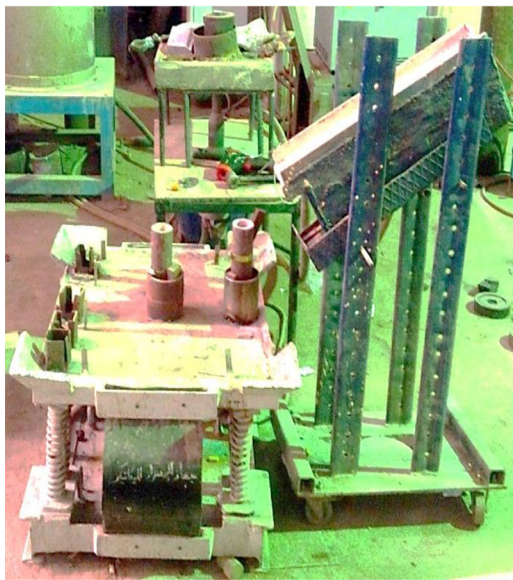


Figure 1. CSP unit with the mold vibration setup and the schematic illustration.

Cooling slope plate is constructed of rectangular iron plate with a groove to allow melt flow.²³ Two holes were drilled through the plate on the bottom side to circulate the water on the cooling plate. The plate length was 500 mm and was inclined by 60° relative to the floor. The plate was coated with a refractory zirconia prior to pouring to prevent melt

adhesion and facilitate separation of the crystals precipitates.

A mechanical vibrator which consists of a motor fixed to the holding table supported by a group of springs was used. The applied frequency and amplitude were kept constant at

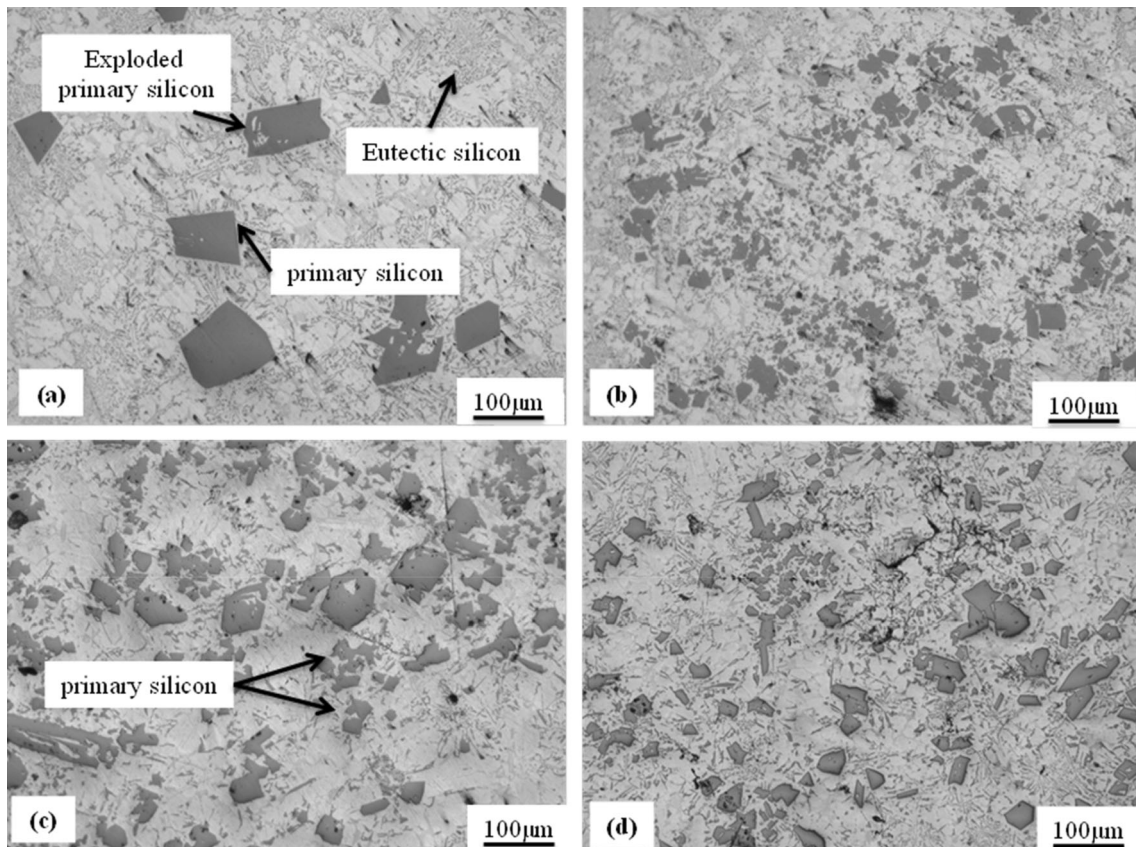


Figure 2. Optical micrographs of metallic mold (a) conventional casting, Reference 22 (b) CSP casting, Reference 22 (c) conventional casting with mold vibration and (d) CSP casting with mold vibration.

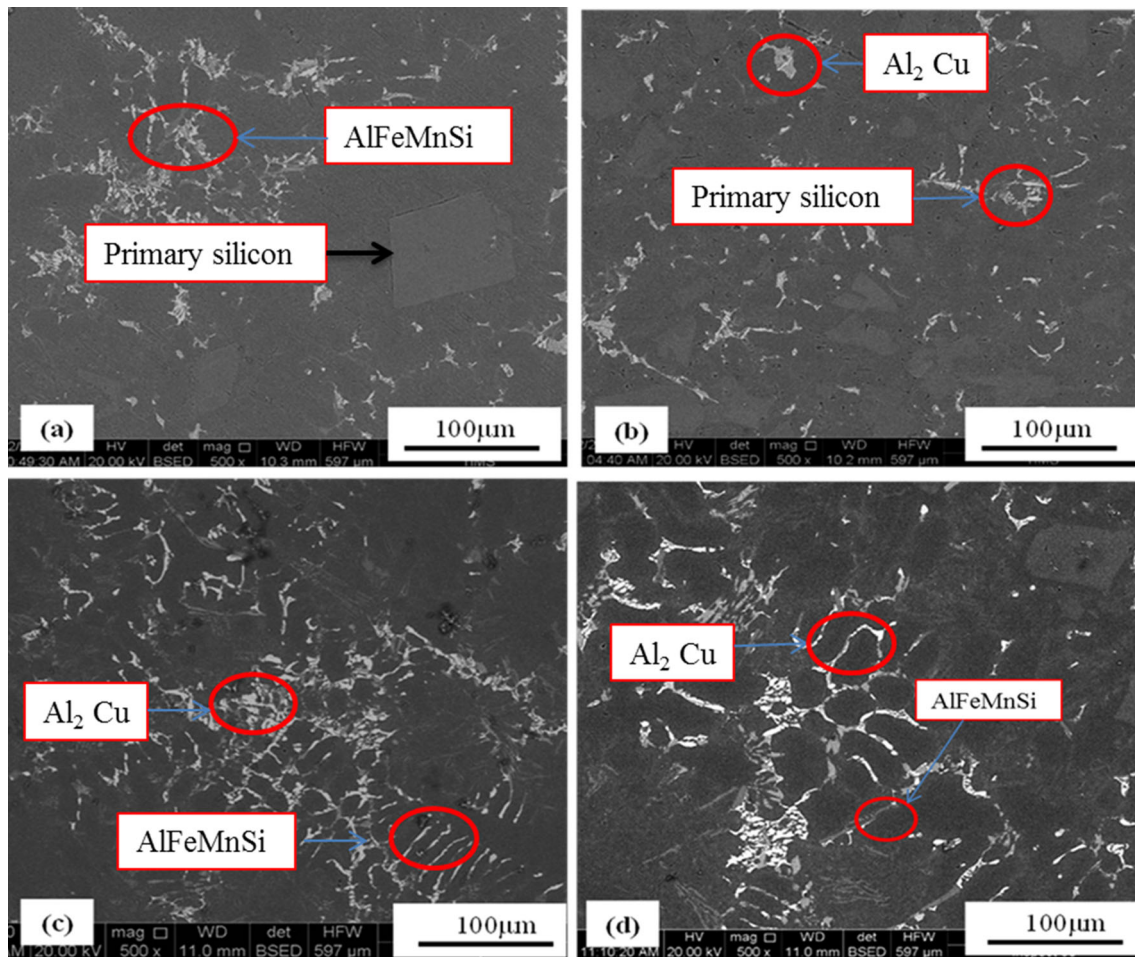


Figure 3. SEM of intermetallic phase in A390 alloy using the metallic mold: (a) conventional casting, (b) CSP casting, (c) conventional casting with mold vibration and (d) CSP casting with mold vibration.

50 Hz and 900 μm during pouring and till solidification. The schematic sketch of the experimental set up is shown in Figure 1.

The molten metal was poured onto the slope plate and the melt cools down and becomes slurry at the end of the plate. The slurry then fills the vibrating mold (metallic or sand), and the vibration was held for 3 min starting from pouring till solidification. Some samples were prepared by conventional casting at the same pouring temperatures used for CSP casting and the same mold vibration conditions for comparison.

Specimens for microstructure investigation were prepared by cutting and grinding using silicon carbide abrasive disks up to 1200 grit followed by polishing with alumina paste. Etching was done using (3% hydrochloric acid (HCl), 5% nitric acid (HNO₃) and 2% hydrofluoric acid (HF) solution.

For the purpose of quantitative analysis of the microstructure features, the specimens were examined by a computerized optical microscope. A scanning electron microscopy (JSM-7000F FEGSEM) combined with back-scattered electrons

(BSE) unit was also used to analyze the different phases and perform elemental mapping. The quantitative image analysis was carried out by image j software according to ASTM E1245 standard, where the Si particle size is defined as $(PSPs) = \left(\frac{4A}{\pi}\right)^{1/2}$, degree of sphericity (DOS) as $\frac{4A}{P^2}$ and volume fraction = $\frac{4P}{\pi A}$. Here, the letter (A) is the area of a silicon particle and (P) the perimeter.

In order to evaluate the mechanical properties, hardness and wear tests were carried out. Hardness was measured by Vickers hardness tester using 10 KN load for 15 s, and the results were the average of five readings. The resistance to wear was evaluated using a pin-on-disk-type wear-test tribometer (T-01 M), where the pin represents the test piece of material and disk material was tool steel disk of 65 HRC. Wear test was conducted at a sliding speed = 0.4 m/s, normal load = 30 N and a constant sliding distance = 2000 m. All the pin specimens were cut with dimensions of (8 × 7 × 7 mm). The samples were cleaned and weighed before and after the test, and the average weight loss of three tests was calculated for each condition. The value of friction force was monitored during the test through a data acquisition system stored in a PC, which enables the calculation

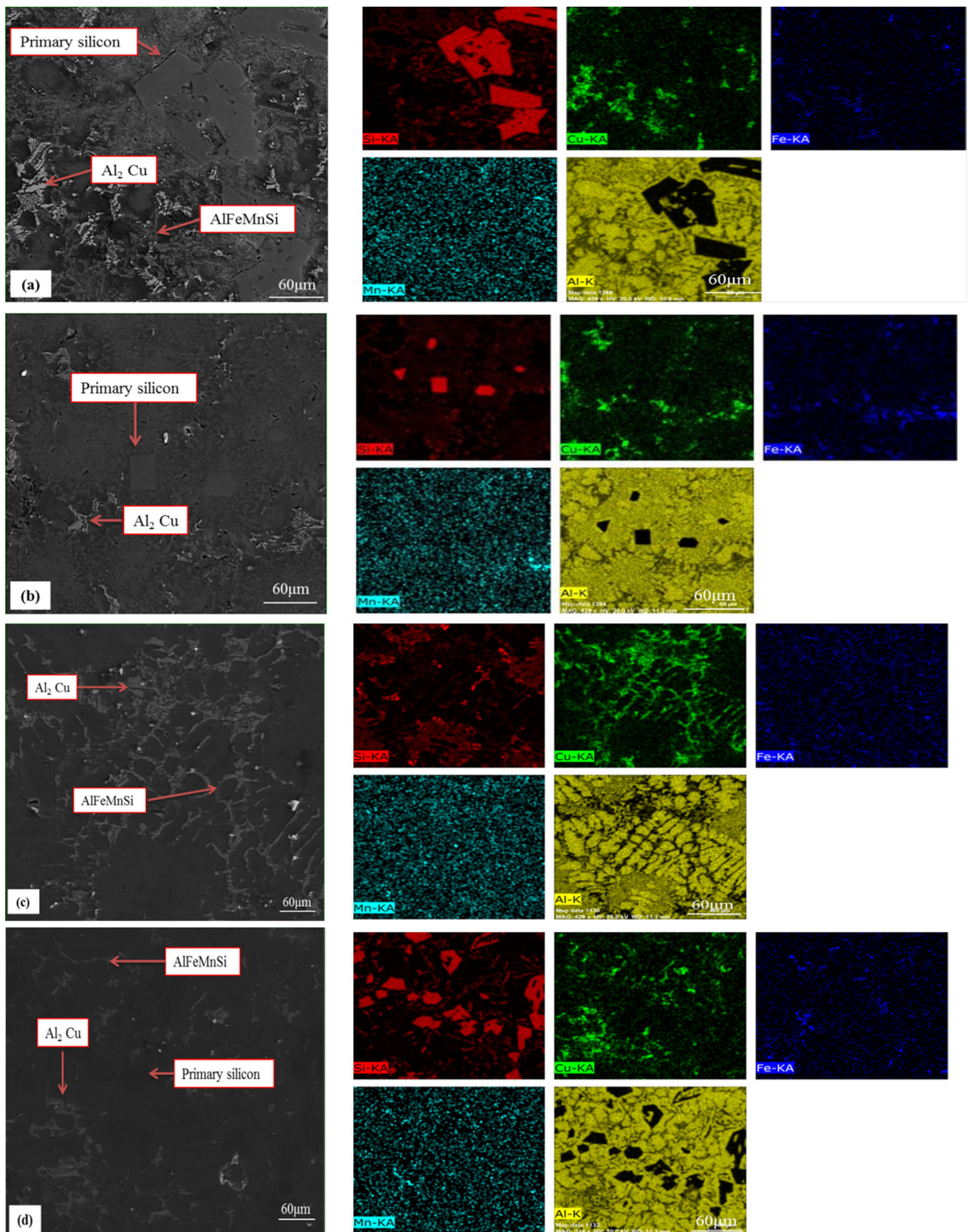


Figure 4. SEM micrographs and EDX elemental mapping of the intermetallic phase in A390 alloy using the metallic mold (a) conventional casting,²² (b) CSP casting,²² (c) conventional casting with mold vibration and (d) CSP casting with mold vibration.

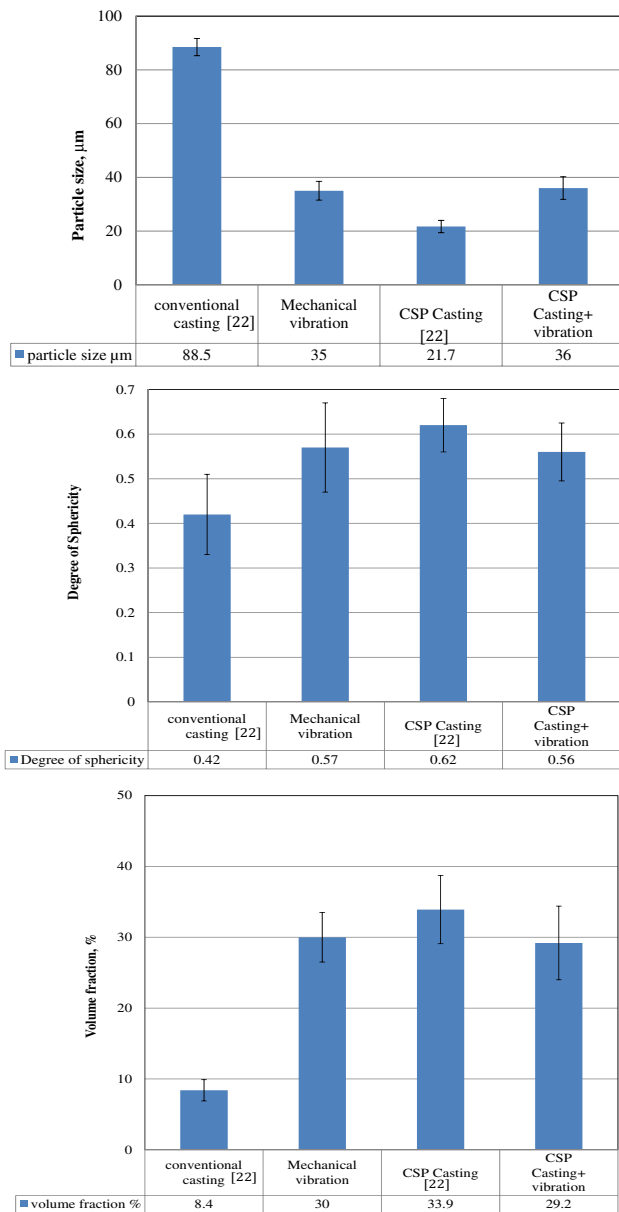


Figure 5. Variations in the particle size, degree of sphericity and volume fraction of the primary silicon particles at different processes in metallic molds.

of friction coefficient as the friction force divided by the actual force (30 N). Wear rate λ was calculated with the following equation $\lambda = \frac{m}{\rho L}$,²⁴ where m is the mass loss, ρ is the density (2.62 g/cm³) and L is the sliding distance.

Results and Discussion

Metallic Mold

Microstructure Investigation

In the conventionally cast samples, the molten alloy is poured directly into the metallic mold. Primary silicon in this case exhibits coarse plate and polygonal shape

morphologies along with large particle size ($\sim 88 \mu\text{m}$). Moreover, unmodified eutectic silicon is also observed, Figure 2a. The microstructure of the castings by mold vibration at the pouring temperature of 690 °C is shown in Figure 2c. It can be observed that applying the mechanical vibration increased the nucleation sites by fragmentation of the solids which leads to refinement of primary silicon with 35 μm , primary silicon exhibits polyhedral like morphology.

Casting using the CSP method could successfully refine the primary Si particles with $\sim 21 \mu\text{m}$ and change the primary silicon morphology to regular and polyhedral shape at the optimum pouring temperature 690 °C shown in Figure 2b. The combined effect of CSP casting with mold vibration showed less refinement of the primary silicon with 36 μm compared to the static mold, as shown in Figure 2d.

The other microstructural features obtained in the cast samples are shown in the SEM micrographs (Figure 3) and their corresponding EDX and elemental mapping (Figure 4). It is clear that the Al₂Cu phase segregates as large clusters, needle-like morphology AlFeMnSi intermetallic phases in case of the conventional casting as clear from Figure 3a. CSP casting has great effect on Al₂Cu and Fe intermetallic phases which were homogeneously dispersed as shown in Figures 3b and 4b.

By applying vibration to the conventional casting, refinement of Al₂Cu and AlFeMnSi intermetallic phase was observed with enhanced morphology and good distribution as shown in Figures 3c and 4c. On the other hand, the combined effect of CSP casting and mold vibration affected the refinement of Al₂Cu intermetallic and redistributed them on the grain boundary, but AlFeSiMn intermetallic exhibited longer needle-like morphology as shown in Figure 3d.

The calculated particle size of primary Si, degree of sphericity and volume fraction as a function in different processes are shown in Figure 5. Following the quantitative analysis of the microstructure features shown in this figure, it is apparent that the primary Si in case of CSP becomes smaller in size from $\sim 88 \mu\text{m}$ for the conventional casting to $\sim 21 \mu\text{m}$ at 690 °C along with regular and polyhedral shape with DOS = 0.62. By application of mold vibration, PSPs decreased to 35 μm with regular and star-like shape with DOS = 0.57. The combined effect of CSP casting with mold vibration resulted in particle size of 36 μm with regular shape with DOS 0.56. The volume fraction distribution of primary Si (defined in ASTM E1245 as number of particles per unit area) followed a typical reverse trend of the particle size, where the volume fraction of primary Si changed from 8.4% for the conventionally cast samples to 30% for vibrated mold and then reduced again to 29.2% with combined effect of CSP casting and mold vibration.

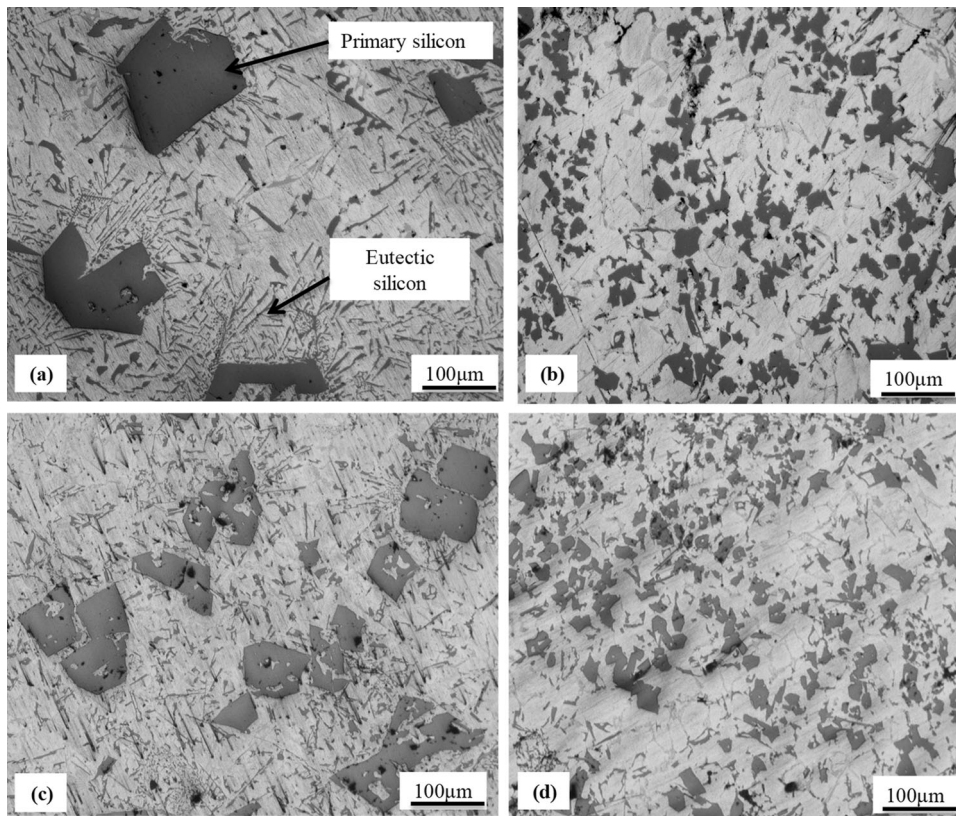


Figure 6. Optical micrographs of sand mold (a) conventional casting,²² (b) CSP casting,²² (c) conventional casting with mold vibration and (d) CSP casting with vibrating sand mold.

The Sand Mold

Microstructure Investigation

Figure 6 shows the optical microstructure at the different processing conditions using the sand mold. The corresponding measurements of Si particles' size, DOS and volume fraction distribution are shown in Figure 7. The conventionally cast alloy exhibited complex microstructure where primary silicon has large particle size ($\sim 184 \mu\text{m}$) with coarse plate and irregular shape morphology with $\text{DOS} = 0.39$ as remarked in Figure 6a. Application of vibration for sand mold noticeably reduced the Si particle size to $\sim 70 \mu\text{m}$ with different morphologies and irregular shapes as obvious from Figure 6c. In the rheo-cast (CSP) samples, Figure 6b, the primary silicon particle size was ($\sim 30 \mu\text{m}$) with fine morphology and regular shape and $\text{DOS} = 0.48$. Unlike the case of the metallic mold, using vibration treatment along with CSP reduced the size of primary silicon to ($\sim 20 \mu\text{m}$) and the primary Si became finer with regular, polyhedral shape with DOS (0.61). Among all the conditions, using the CSP method with the mold vibration could successfully refine the primary Si particles and alters their distribution compared to other different process.

The other microstructural features obtained in the sand cast samples are shown in the SEM micrographs and their corresponding EDX analysis of Figure 8. It is clear that the Al_2Cu intermetallic segregates as large clusters in case of the conventional casting and vibration treatment, Figure 8a, c while it is homogeneously dispersed in the matrix as fine particles after CSP casting, Figure 8b. By CSP casting with vibration, Al_2Cu intermetallic phase became finer and distributed around the grain boundaries, Figure 8d. Another important microstructure feature which can be detected from the EDX elemental mapping of Figure 9 is Fe intermetallic (AlFeSiMn , AlFeSi) which appeared as coarse plate, needle-like shape and segregated in some areas in conventional casting and vibration treatment.²⁵ In case of casting using the CSP and CSP with mold vibration, the morphology of Fe intermetallic was enhanced. It was reported that the coarse platelet like AlFeMnSi phases can deteriorate the mechanical properties of Al-Si alloys by acting as potential sites of crack initiation.^{26,27} Several research works were done in order to decrease the size or alter the shape of this type of intermetallic phases.^{16,28} The fragmented AlFeMnSi phase is believed to affect the mechanical properties of the CSP and CSP casting with vibration cast samples.

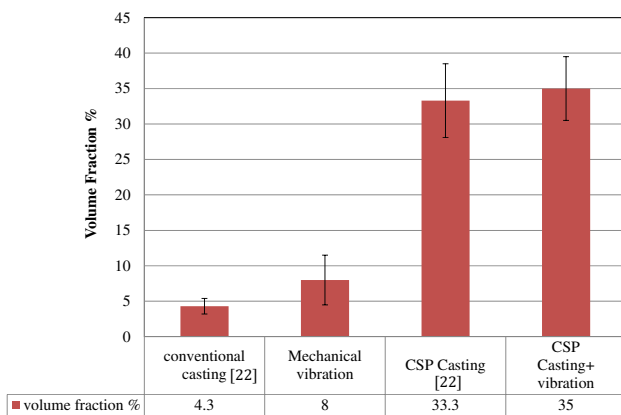
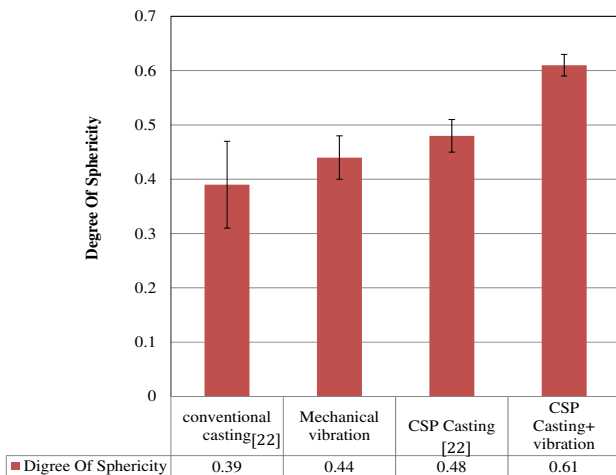
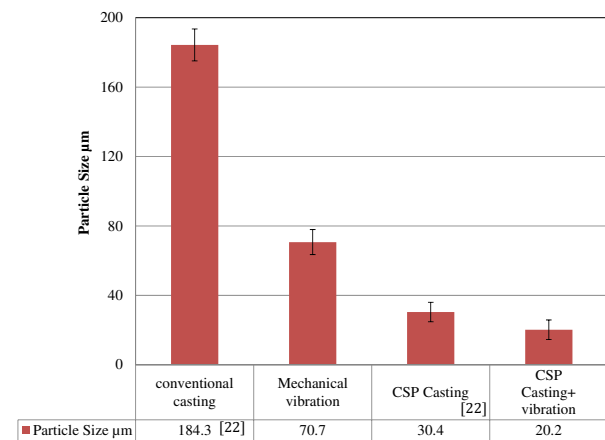


Figure 7. Variations in the particle size, degree of sphericity and volume fraction of the primary silicon particles at different process in the sand mold.

Solidification Mechanisms

CSP Casting Process

In case of CSP casting, during the first stage of solidification, the primary silicon nucleates on the surface of the plate due to the low solubility of silicon and the difference

of densities between Si grains (2.33 g/cm^3) and liquid matrix (2.62 g/cm^3) and also due to the forced convection between the molten metal and the wall of the inclined plate.²⁹

In the second step of all the rheo-casting processes, the convection creates high undercooling levels and the copious nucleation is the responsible for increasing the nucleation rate of primary Si phase which cause a high grain density. A high grain density, i.e., large number of grains “nuclei” during the initial stages of solidification of an alloy melt, results in increasing of the volume fraction of Si.³⁰ The shear stress and the turbulence which are both caused by the accelerated melt flow on the CSP separate, fragment and distribute the primary silicon into the melt and restrict its growth. In the final stage, this strong melt flow washes away the non-dendritic structures in the shape of slurry which is poured into the mold for complete solidification as illustrated in Figure 10.

Effect of Mold Vibration

Solidification under mold vibration conditions can be explained as follows: In the first stage, heterogeneous nucleation of primary Si happens on the mold surface due to the forced convection generated by the vibration energy.³¹ The turbulent flow then produces waves that separate the nucleus from the mold wall at a later stage and nucleus collision takes place. Afterward, the destroyed nucleus moves toward the center of casting and acts as a nucleation site for creation of new grains which subsequently causes crystal multiplication and increases the nucleation rate³² as illustrated in Figure 11.

The Combined Effect of CSP Casting and Mechanical Vibration

In the current experiments where a vibrating mold is used, the solidification process occurs through two steps; the first one is the partial solidification on the static cooling slope plate, and the second step is the dynamic solidification inside the cavity of the vibrating mold as illustrated in Figure 12. It is believed here that microstructure formation follows the routes summarized in Figure 13 where three mechanisms devote to nucleus formation, namely heterogenous nucleation, eruptive nucleation and nucleus multiplication.^{8,33} During the first stage of solidification (on the CSP), heterogenous and copious nucleation occur on the plate thus producing large quantity of nuclei on the plate surface due to the forced convection, and the shear force then separates the

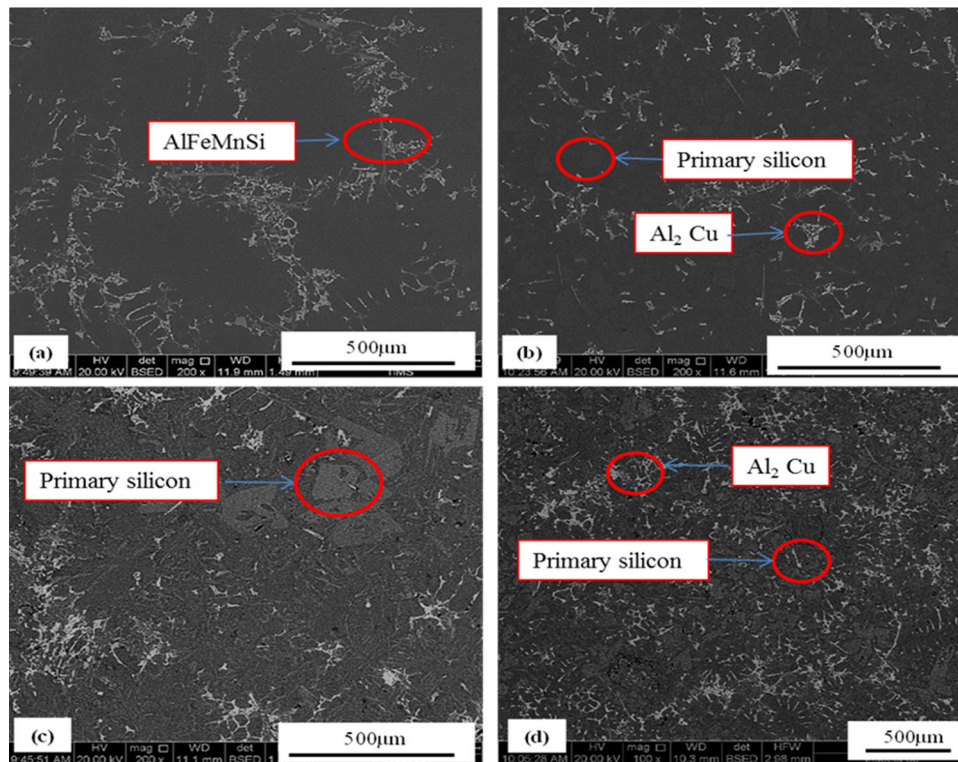


Figure 8. SEM micrographs of intermetallic phase in A390 alloy using the sand mold: (a) conventional casting²², (b) CSP casting²², (c) conventional casting with mold vibration and (d) CSP casting with mold vibration.

primary silicon particles from the plate and wash it away with the melt (slurry) flow.³⁴

This slurry with the non-dendritic structure which is formed at the end of the plate due to the controlled nucleation completes the solidification process under the influence of mold vibration. According to^{32,35–37}, mold vibration can accelerate the elements diffusion velocity and distribute the solutes uniformly and hence results in eruptive nucleation in the whole melt. Simultaneously, the vibration causes crystal multiplication by increasing the effective nucleus and induces a viscous drag force which causes nucleus detachment on the mold wall. The detached particles become new sources of nucleation thus increasing nucleation rate.³⁸

In case of CSP casting in metallic mold, the mold increases the cooling rate and hence increases the speed of solidification process by decreasing the solidification time, and therefore, there is no chance for the mechanical vibrations to play its role in increasing the nucleation rate. Contrasting, in case of CSP casting in a vibrating sand mold, fine and uniformly distributed primary silicon could be achieved.

Mechanical Properties Evaluation

Hardness

Figure 14 shows the hardness measurements of the samples solidified in metallic and sand molds using different processes. For the metallic mold, the pre-mentioned reduction in the average particle size and the uniform distribution of Si particles and the other observed microstructure features increased the hardness from 95.3 Hv in conventional casting to 111 Hv for vibration treatment in liquid state, and this value was further enhanced to 114.6 Hv by using the CSP casting and then decreased to 110 Hv by applying vibration in semisolid state. For the sand mold specimens, hardness was increased from 89 Hv in conventional casting to 98 Hv and 113 Hv using mold vibration and CSP, respectively. Furthermore, the optimum hardness of 115 Hv was obtained due to using the combination of CSP and mold vibration. These differences in hardness are strongly correlated with the primary Si shape and distribution shown in Figures 2 and 6.

In case of the conventional casting, applying vibration to the molten metal in the liquid state, vibration increases the

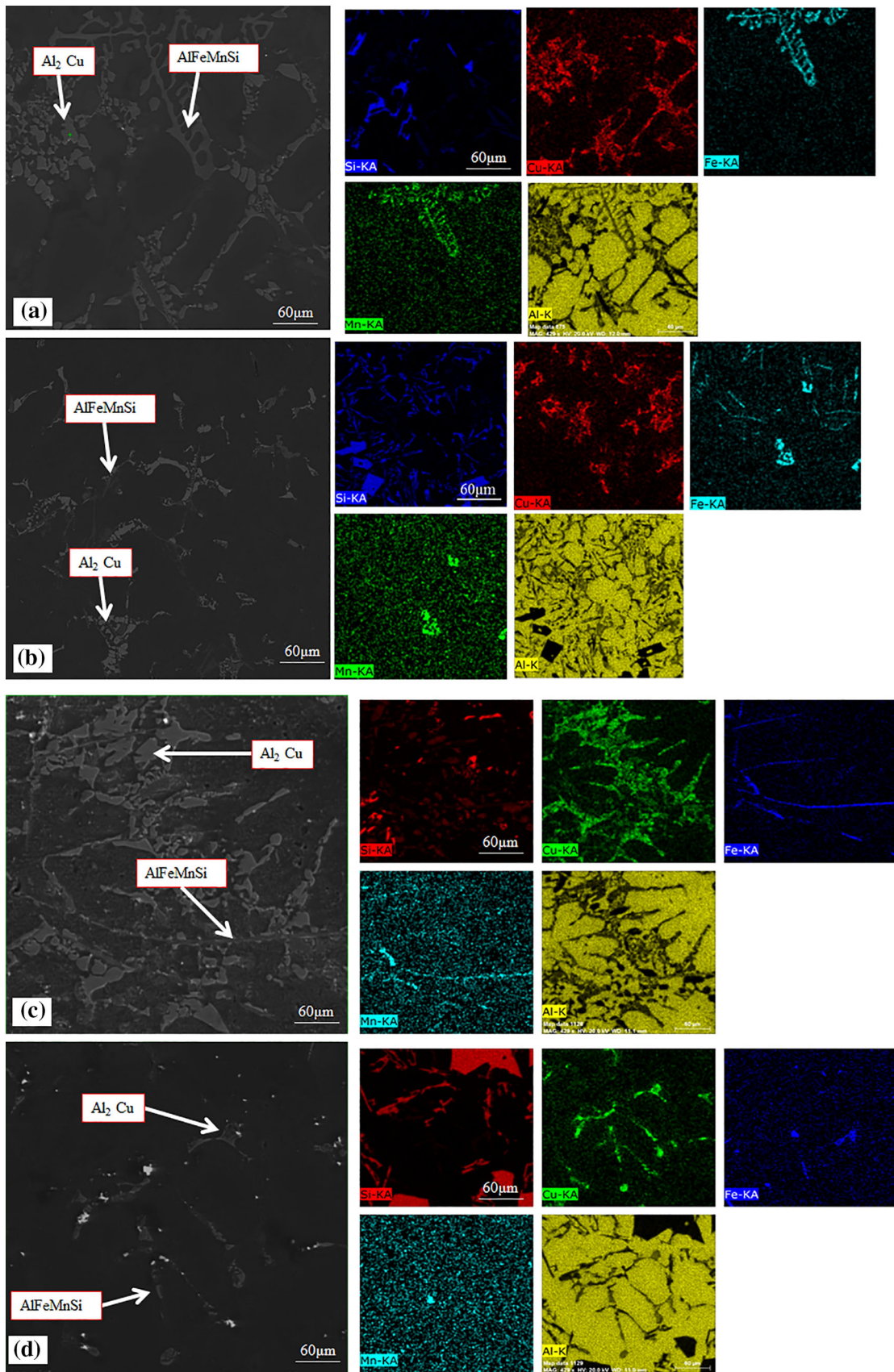
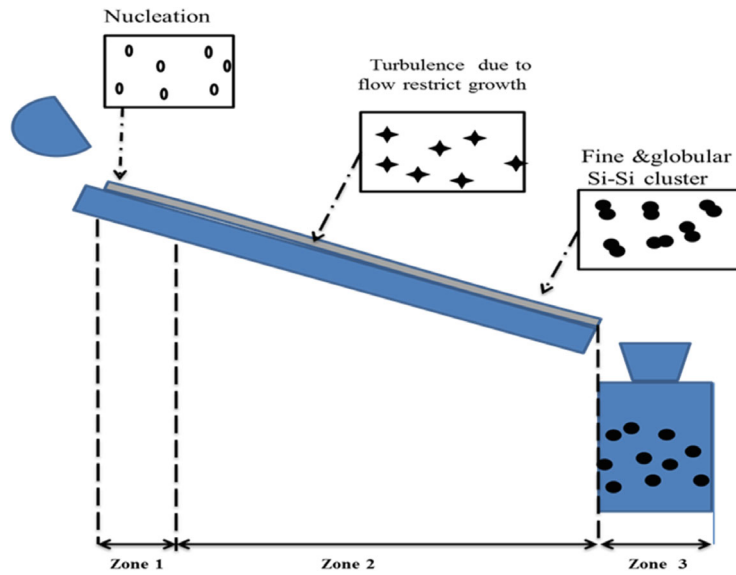


Figure 9. SEM micrographs and EDX elemental maps of intermetallic phase in A390 alloy using the sand mold: (a) conventional casting,²² (b) CSP casting,²² (c) conventional casting with mold vibration and (d) CSP casting with mold vibration.



Cooling slope plate			Mold
Partial solidification			Complete solidification
Heterogeneous Nucleation	Copious nucleation & shearing	Restricted Growth by turbulence	Cooling rate
Zone 1	Zone 1,2	Zone 2	Zone 3

Figure 10. Solidification and refinement mechanisms by using CSP casting.

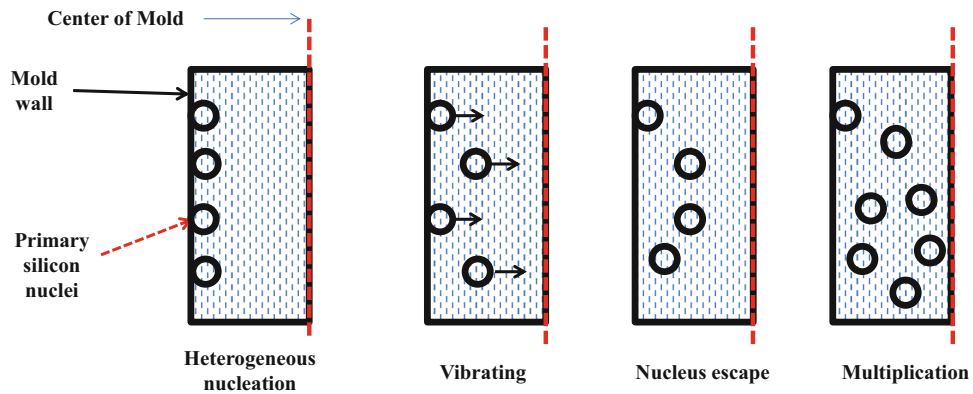
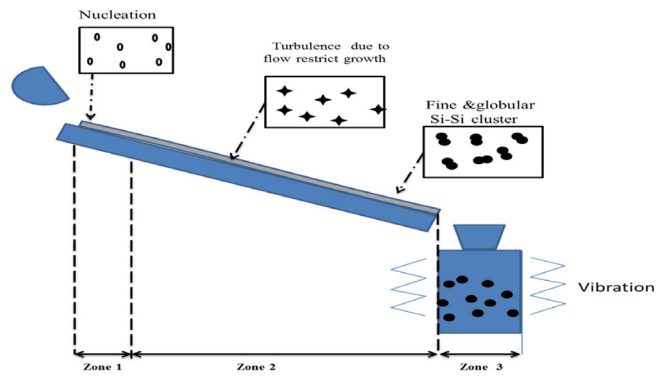


Figure 11. Dynamic solidification & refinement mechanisms on liquid state³⁷.



Cooling slope plate			Vibrated Mold
Partial solidification			Complete solidification
Heterogeneous Nucleation	Copious nucleation & shearing	Restricted growth by turbulence	Eruptive nucleation & Crystal multiplication
Zone 1	Zone 1,2	Zone 2	Zone 3

Figure 12. Solidification process by using CSP casting with vibrating mold.

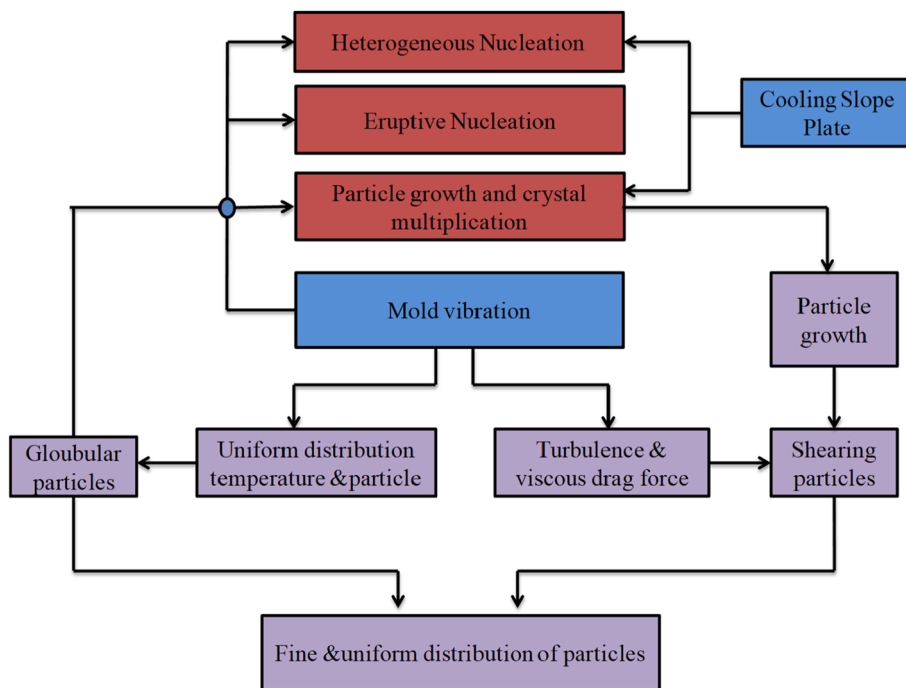


Figure 13. Routes of solidification process during CSP with vibrating mold³².

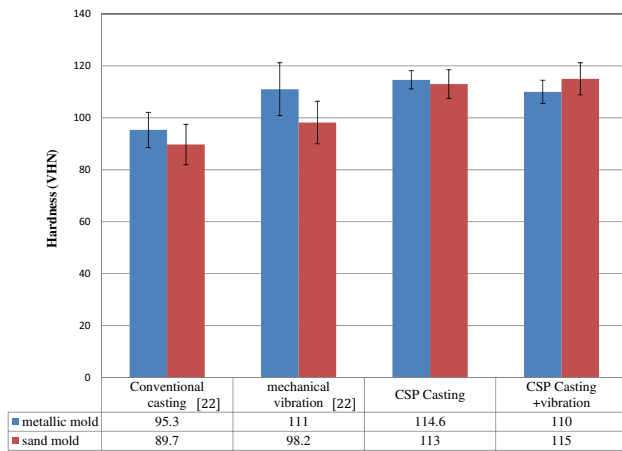


Figure 14. Hardness variation using different processes compared to the conventional casting.

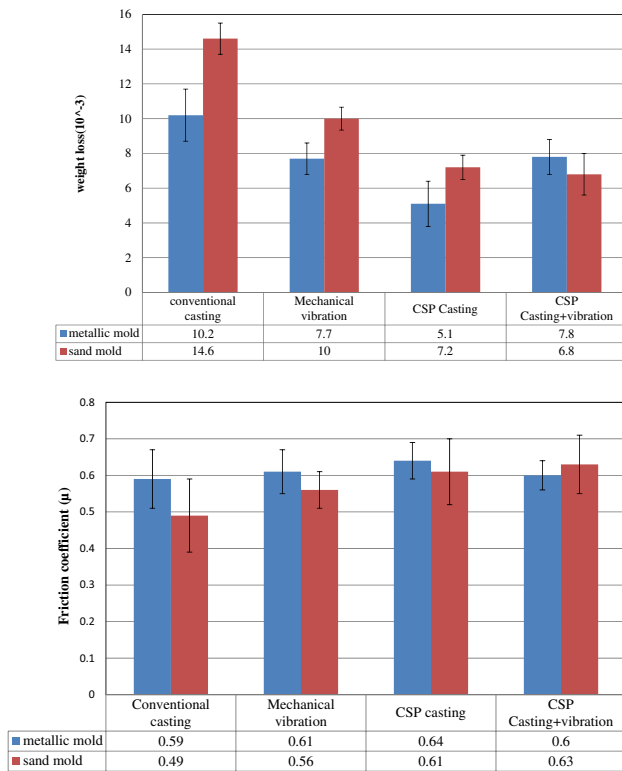


Figure 15. Variations in the weight loss and friction coefficient at different processes for metallic and sand molds.

nucleation rate and the metallic mold increases the cooling rate and restricts the particles growth rate and this contributes to the increase in hardness. In CSP casting in metallic mold, vibration was not effective enough due to the short solidification time of the slurry inside the mold which decreases the effectiveness of vibration. In CSP casting in sand molds, there is enough time for the vibrations to occur due to the slower solidification rate in the sand mold, and therefore, fine microstructure was observed and hence enhanced mechanical properties.

Wear Resistance

Figure 15 shows the tribological performance in terms of weight loss and friction coefficient. It can be seen that CSP casting achieved lower weight loss and higher friction coefficient compared to the conventionally cast specimens. On the other hand, sand mold CSP casting with vibration achieved lower weight loss and higher friction coefficient compared to CSP casting in a vibrating metallic mold. Based on previous microstructure analysis, the structure with refined primary Si could successfully reduce the crack tendency and improve wear resistance. Furthermore, the refinement and homogenization of the present intermetallic particles which act as effective load-bearing elements were beneficial in enhancing the wear resistance since they have good interfacial bonding with the matrix. Besides, the fragmentation of the coarse Fe intermetallic particles decreased the chance of the localized failure while moving in contact with the counter disk. The increased values of friction coefficient, shown in Figure 15, confirm these observations. The coefficient of friction is proportionally related to the friction force^{38,39}, and hence, the harder the sample the higher is the friction force (considering the same counter disk) and the larger is the friction coefficient.

In order to investigate the wear mechanism, the worn surfaces were examined under SEM and the results are shown in Figures 16 and 17. The worn surface of the conventionally cast alloy shows more damage, Figures 16a and 17a, due to the heavy plastic deformation of the surface layer which causes heating of the worn surface and makes the alloy softer. On the other hand, CSP specimens showed lower distortion on the edges of the tracks, some slightly curled-up layers could be observed, but inside the tracks,

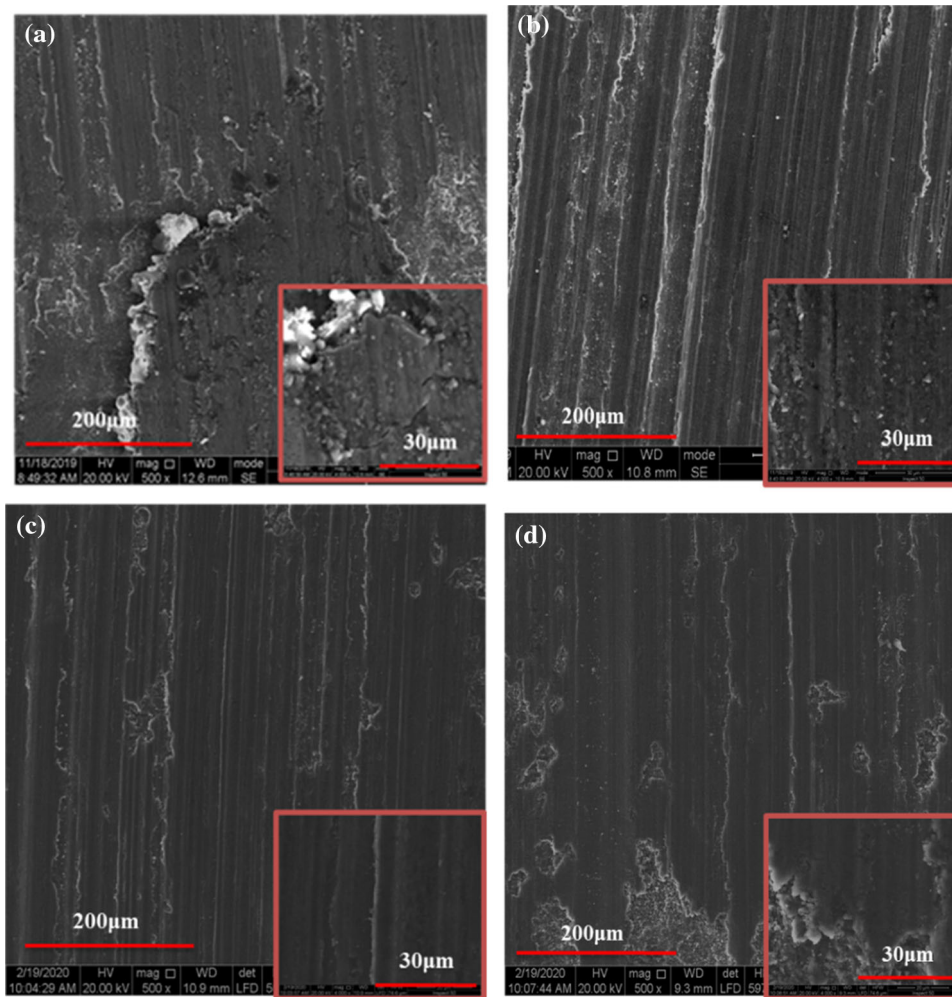


Figure 16. Worn surface morphology of the samples poured in metallic mold where (a) conventional casting Reference,²² (b) CSP Reference,²² (c) conventional casting with mold vibration and (d) CSP with mold vibration.

the surfaces were very smooth compared to the conventional casting as clear from Figures 15b and 16b. The worn surface of vibration treatment exhibited similar continuous parallel wear tracks with small width (34 µm). By CSP casting with vibration, there were finer plowing grooves, larger wear track width (85 µm) and layers of material were removed with severe wear.

According to Ojha et al.³⁹ and Anasyida et al.⁴⁰, presence of coarse secondary phase particles in the microstructure which do not have enough bonding with the matrix creates interfacial areas that become then sites for micro-cracking upon exposure to friction loading. This means the larger the particle size, the higher chance for micro-cracking during the wear test.

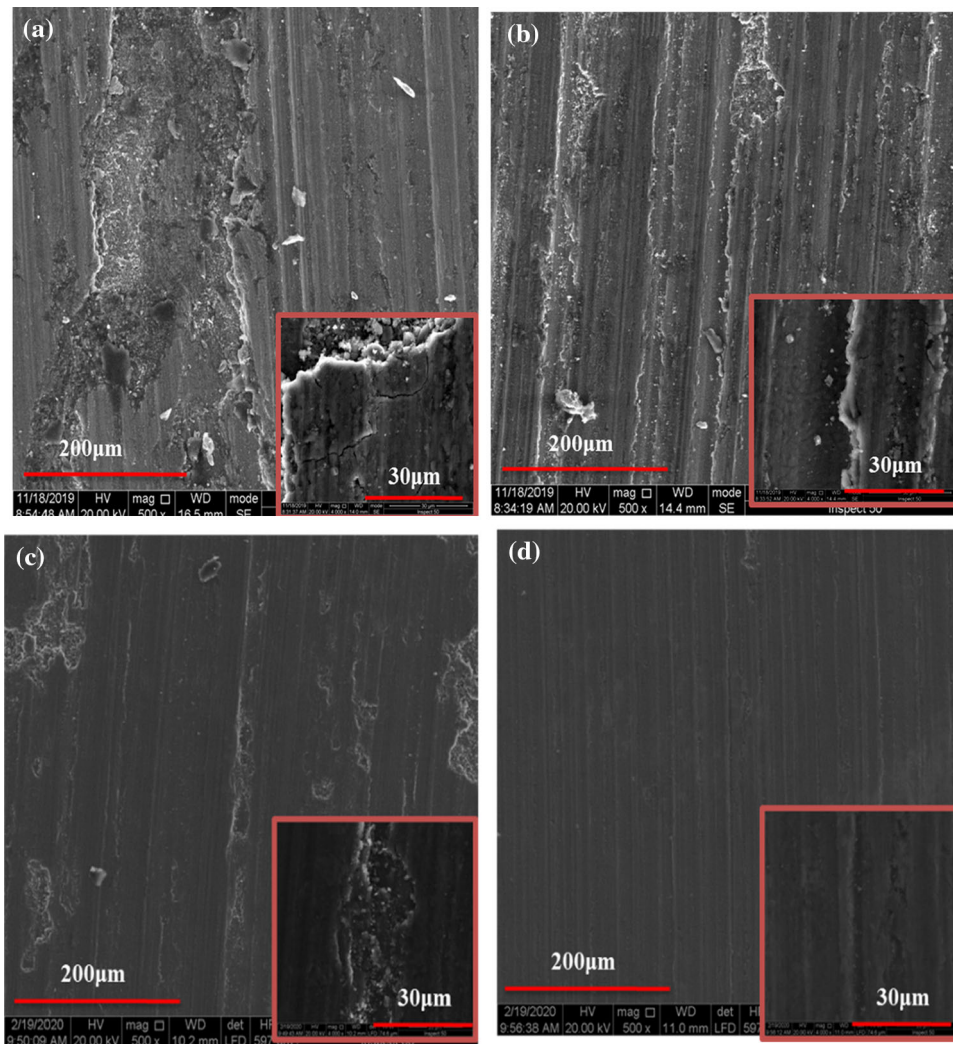


Figure 17. Worn surface morphology of the samples poured in sand mold where (a) conventional casting,²² (b) CSP,²² (c) conventional casting with mold vibration and (d) CSP with mold vibration.

Conclusions

The combined effects of cooling slope plate casting with mold vibration on the microstructure, hardness and wear resistance of hypereutectic Al–Si alloy (A390) were investigated, and the following conclusions were driven:

1. Microstructure refinement including fine and uniformly distributed primary Si, along with modified Al_2Cu phase and fragmented Fe-intermetallic particles can be obtained by CSP sand casting integrated with mechanical mold vibration.
2. Mechanical vibration in case of CSP casting in the metallic mold is not effective in terms of microstructure refinement.
3. Cooling slope casting integrated with the sand mold vibration causes increase in the hardness and improvement in the wear properties of alloy

A390 by decreasing the size of primary Si to 70%, increasing the hardness by 20% and decreasing weight loss by 50% compared to the conventional casting.

Acknowledgements

The authors would like to thank the financial support from The Central Metallurgical Research and Development Institute, Grant No. 146/2019. The corresponding author would like to acknowledge the partial support from the Science and Technology Development Fund (Egypt) through the Grant No. 26565.

REFERENCES

1. L. Lasa, J.M. Rodriguez-Ibab, Wear behaviour of eutectic and hypereutectic Al–Si–Cu–Mg casting

- alloys tested against a composite brake pad. *Mater. Sci. Eng. A* **363**, 193–202 (2003)
2. H. Tahiri, A.M. Samuel, H.W. Doty et al., Effect of Sr–Grain Refiner–Si interactions on the microstructure characteristics of Al–Si hypereutectic alloys. *Int. J. Metalcast.* **12**, 307–320 (2018). <https://doi.org/10.1007/s40962-017-0164-5>
 3. Q. Li, B. Li, J. Liu et al., Modification of hypereutectic Al–20 wt% Si alloy based on the addition of yttrium and Al–5Ti–1B modifiers mixing melt. *Int. J. Metalcast.* **13**, 367–383 (2019). <https://doi.org/10.1007/s40962-018-0242-3>
 4. R.G. Guan, D. Tie, A Review on grain refinement of aluminum alloys: progress, challenges and prospects. *Acta Metall. Sin.* **30**, 409–432 (2017)
 5. C. Limmaneevichitr, S. Pongananpanya, J. Kajornchaiyakul, Metallurgical structure of A356 aluminum alloy solidified under mechanical vibration: an investigation of alternative semi-solid casting routes. *Mater. Des.* **30**, 3925 (2009)
 6. F. Taghavi, H. Saghafian, Y.H.K. Kharrazi, Study on the effect of prolonged mechanical vibration on the grain refinement and density of A356 aluminum alloy. *Mater. Des.* **30**, 1604 (2009)
 7. H.M. Guo, A.S. Zhang, X.J. Yang, M.M. Yan, Grain refinement of Al–5%Cu aluminum alloy under mechanical vibration using melt able vibrating probe. *Trans. Nonferrous Metal. Soc.* **24**, 2489 (2014)
 8. N.K. Kund, Effect of tilted plate vibration on solidification and microstructural and mechanical properties of semisolid cast and heat-treated A356 Al alloy. *Int. J. Adv. Manuf. Technol.* **97**, 1617–1626 (2018)
 9. S.G. Shabestari, M. Ghanbari, Effect of plastic deformation and semisolid forming on iron–manganese rich intermetallic in Al–8Si–3Cu–4Fe–2Mn alloy. *Alloys Compd.* **508**, 315–319 (2010)
 10. W. Khalifa, S. El-Hadad, Y. Tsunekawa, Microstructure and wear behavior of solidification sonoprocessed B390 hyper-eutectic Al–Si alloy. *Metall. Mater. Trans. A* **44**, 5817–5824 (2013)
 11. K. Liu, X. Cao, X.G. Chen, Solidification of iron-rich intermetallic phases in Al–4.5Cu–0.3Fe cast alloy. *Metall. Mater. Trans. A* **42**, 2004–2016 (2011)
 12. D.N. Miller, L. Lu, A.K. Dahle, The role of oxides in the formation of primary iron intermetallics in an Al–11.6Si–0.37 Mg alloy. *Metall. Mater. Trans. B* **37**, 873–878 (2006)
 13. J. Barbosa, H. Puga, J. Oliveira, S. Ribeiro, M. Prokic, Physical modification of intermetallic phases in Al–Si–Cu alloys. *Mater. Chem. Phys.* **148**, 1163–1170 (2014)
 14. W. Khalifa, Y. Tsunekawa, S. El-Hadad, Ultrasonic rheo-die casting of A383 aluminum alloy. *Solid State Phenom.* **256**, 282–287 (2016)
 15. S. Wu, S. Lu, P. An, Z. Zhu, Preparation and rheocasting of semi-solid aluminum alloy slurry with indirect ultrasonic vibration process. *MRS Proc.* **1380**, 1380 (2012)
 16. W. Khalifa, S. El-Hadad, Ultrasonication effects on the microstructure characteristics of the A380 die cast alloy. *Int. J. Metalcast.* **13**, 865–879 (2019). <https://doi.org/10.1007/s40962-018-00296-8>
 17. S. Wu, S. Lu, P. An, H. Nakae, Microstructure and property of rheo-casting aluminium alloy made with indirect ultrasonic vibration process. *Mater. Lett.* **73**, 150–153 (2012)
 18. S. Gencalp, N. Saklakoglu, “effect of low frequency mechanical vibration and casting temperatures on microstructure of semisolid AlSi₈Cu₃Fe alloy. *Arab. J. Sci. Eng.* **37**, 2255–2267 (2012)
 19. P. Das, S.K. Samanta, P. Dutta, Microstructure evolution and rheological behavior of cooling slope processed Al–Si–Cu–Fe alloy slurry. *Miner. Met. Mater. Soc. ASM Int.* **47**, 2243–2246 (2016)
 20. S.D. Kumar, A. Mandal, M. Chakraborty, Cooling slope casting process of semisolid aluminum alloys: a review. *Int. J. Eng. Res. Technol.* **3**, 269–283 (2014)
 21. R.G. Guan, Z.Y. Zhao, H. Zhang, C. Lian, C.S. Lee, C.M. Liu, *J. Mater. Process. Technol.* **212**, 1430 (2012)
 22. M.M. Shehata, S. El-Hadad, M.E. Moussa, M. EL-Shennawy, Optimizing the pouring temperature for semisolid casting of a hypereutectic Al–Si alloy using the cooling slope plate method. *Int. J. Metalcast.* (2020). <https://doi.org/10.1007/s40962-020-00465-8>
 23. M. Ramadan, N. Fathy, Solidification microstructure of rheocast hyper-eutectic Al–18Si alloy. *J. Metall. Eng.* **2**, 149–154 (2013)
 24. Z. Hu, G. Wu, J. Xu, Dry wear behavior of rheocasting Al – 16Si – 4Cu – 0.5 Mg alloy. *Trans. Nonferrous Met. Soc. China* **26**, 2818–2829 (2016)
 25. M. Qi, J. Li, Correlation between segregation behavior and wall thickness in a rheological high pressure die-casting AC46000 aluminum alloy. *J. Mater. Res. Technol.* **8**, 3565–3579 (2019)
 26. M.N. Mohammed, M.Z. Omar, M.S. Salleh, K.S. Alhawari, P. Kapranos, Semisolid metal processing techniques for non-dendritic feedstock production. *Sci. World J.* **2013**, 752175 (2013). <https://doi.org/10.1155/2013/752175>
 27. K.S. Alhawari, M.Z. Omar, M.J. Ghazali, M.S. Salleh, M.N. Mohammed, Evaluation of the microstructure and dry sliding wear behaviour of thixoformed A319 aluminium alloy. *Mater. Des.* **76**, 169–180 (2015)
 28. W. Khalifa, S. El-Hadad, Y. Tsunekawa, Microstructure evolution and mechanical properties of sono processed-Thixo cast AC4C Billets, in *71st World Foundry Congress on Advanced Sustainable Energy*, 19–21 May, Bilbao-Spain (2014)
 29. C. Cui, A. Schulz, K. Schimanski, H.W. Zoch, Spray forming of hypereutectic Al–Si alloys. *J. Mater. Process. Technol.* **209**, 5220–5228 (2009)
 30. R.A. Flemings, M.C. Martinez, Principles of microstructural formation in semi-solid metal processing. *Solid State Phenom.* **116–117**, 1–8 (2006)

31. L.N. Yu, X.F. Liu, H.M. Ding, X.F. Bia, A new nucleation mechanism of primary Si by like-peritectic coupling of AlP and Al₄C₃ in near eutectic Al–Si alloy. *J. Alloys Compd.* **429**, 119–125 (2007)
32. R.G. Guana, F.R. Caoa, L.Q. Chenb, J.P. Lib, C. Wanga, Dynamical solidification behaviors and microstructural evolution during vibrating wavelike sloping plate process. *J. Mater. Process. Technol.* **209**, 2592–2601 (2009)
33. R.G. Guan, Z.Y. Zhao, C.S. Lee, Q.S. Zhang, C.M. Liu, Effect of wavelike sloping plate rheo-casting on microstructures of hypereutectic Al-18% Si-5% Fe alloys. *Miner. Met. Mater. Soc. ASM Int.* (2011)
34. J. Deshpande, The Effect of mechanical mold vibration on the characteristics of aluminum alloys. M.Sc Thesis, Worcester Polytechnic Institute, Manufacturing Engineering, September (2006)
35. J. Campbell, Grain refinement of solidifying metals by vibration: a review, in *Proceedings of the Solidification Technology in the Foundry and Cast House*, Coventry, UK, 15–17 September (1980), pp. 61–64
36. J. Campbell, Effects of vibration during solidification. *Int. Mater. Rev.* **2**, 71–106 (1981)
37. R.D. Doherty, Comments on mechanical deformation of dendrites by fluid flow during the solidification of undercooled melts. *Scripta Mater.* **49**, 1219–1222 (2003)
38. M. Harun, I.A. Talib, A.R. Daud, Effect of element additions on wear property of eutectic aluminium–silicon alloys. *Wear* **194**, 54–59 (1996)
39. K.V. Ojha, A. Tomar, D. Singh, G.C. Kaushal, Shape, microstructure and wear of spray formed hypoeutectic Al–Si alloys. *Mater. Sci. Eng., A* **487**, 591–596 (2008)
40. A.S. Anasyida, A.R. Daud, M.J. Ghazali, Dry sliding wear behavior of Al–12Si–4 Mg alloy with cerium addition. *Mater. Des.* **31**, 365–371 (2010)

Publisher's Note Springer Nature remains neutral with regard to jurisdictional claims in published maps and institutional affiliations.